

Breakdown of electrostatic predictions for the nonlinear dispersion relation of a stimulated Raman scattering driven plasma wave

Didier Bénisti,^{1,a)} David J. Strozzi,² and Laurent Gremillet¹

¹Département de Physique Théorique et Appliquée, CEA/DAM Ile-de-France, Bruyères-Le-Châtel, 91287 Arpajon Cedex, France

²Lawrence Livermore National Laboratory, University of California, Livermore, California 94550, USA

(Received 30 October 2007; accepted 4 February 2008; published online 17 March 2008)

The kinetic nonlinear dispersion relation, and frequency shift $\delta\omega_{\text{SRS}}$, of a plasma wave driven by stimulated Raman scattering are presented. Our theoretical calculations are fully electromagnetic, and use an adiabatic expression for the electron susceptibility which accounts for the change in phase velocity as the wave grows. When $k\lambda_D \geq 0.35$ (k being the plasma wave number and λ_D the Debye length), $\delta\omega_{\text{SRS}}$ is significantly larger than could be inferred by assuming that the wave is freely propagating. Our theory is in excellent agreement with 1D Eulerian Vlasov–Maxwell simulations when $0.3 \leq k\lambda_D \leq 0.58$, and allows discussion of previously proposed mechanisms for Raman saturation. In particular, we find that no “loss of resonance” of the plasma wave would limit the Raman growth rate, and that saturation through a phase detuning between the plasma wave and the laser drive is mitigated by wave number shifts. © 2008 American Institute of Physics.

[DOI: 10.1063/1.2888515]

Currently, there is renewed interest in the nonlinear dispersion relation of electron plasma waves (EPWs), particularly with regards to backward stimulated Raman scattering (SRS) at large $k\lambda_D$ (where k is the EPW wave number and λ_D is the Debye length). For example, Vu *et al.*¹ invoked phase detuning between the plasma wave and the laser drive, a consequence of the nonlinear frequency downshift of the EPW, as a mechanism for Raman saturation and as an explanation for the chaotic behavior of the Raman reflectivity. Brunner and Valeo² proposed the alternative view that the growth of electrostatic sidebands, produced by the trapped particle instability, is at the origin of Raman saturation and burstiness. Rose and Russell³ found a critical wave amplitude, $\Phi_{\text{max}}(k\lambda_D)$, beyond which there is no solution to the dispersion relation of a free EPW, and called this a “loss of resonance.” They further showed (see Ref. 4) that this feature strongly limits the growth of SRS, especially when $k\lambda_D > 0.53$ since $\Phi_{\text{max}}=0$ for $k\lambda_D > 0.53$.

In this Letter we provide a theoretical estimate, $\delta\omega_{\text{SRS}}$, for the frequency shift of an SRS-driven EPW, derived within the context of the three-wave model where the total electric field is

$$\vec{E}_{\text{tot}} = E_p \sin(\varphi)\hat{x} + [E_l \sin(\varphi) + E_s \cos(\varphi_s)]\hat{y}. \quad (1)$$

E_p , E_l , and E_s are slowly varying non-negative envelopes for, respectively, the plasma, laser, and scattered waves. The electromagnetic wave numbers and frequencies are given by $k_{l,s} = \partial_x \varphi_{l,s}$ and $\omega_{l,s} = -\partial_t \varphi_{l,s}$. Those of the plasma wave are $k = \partial_x \varphi$ and $\omega = -\partial_t \varphi$. The phase shift between the laser drive and the plasma wave is $\delta\varphi \equiv \varphi + \varphi_s - \varphi_l$. As shown in Ref. 5, at zero order in $k^{-1} \partial_x E_p$, the fully electromagnetic EPW dispersion relation is

$$1 + \alpha_d \text{Re}(\chi) = 0, \quad (2)$$

where χ is the electron susceptibility defined by Eq. (11) of Ref. 5 and where

$$\alpha_d \equiv \frac{1 + 2\eta^{-1} \sin(\delta\varphi) + \eta^{-2}}{1 + \eta^{-1} \sin(\delta\varphi)}. \quad (3)$$

$\eta \equiv E_p/E_d$, $E_d \equiv (kv_{os}/2\omega_s)E_s$ is the amplitude of the ponderomotive field due to the laser drive, and $v_{os} \equiv eE_l/(m\omega_l)$. From Eq. (3), one recovers that the dispersion relation of a free wave is given by Eq. (2) with $\alpha_d=1$. Figures 1 and 2 show that when $k\lambda_D \geq 0.35$, we find that the frequency shift for a free wave, $\delta\omega_{\text{free}}$, decreases more slowly with $\Phi \equiv eE_p/kT_e$ than $\delta\omega_{\text{SRS}}$, which we explain as follows. When solving Eq. (2), we assume that the linear value of the driven EPW frequency, $\omega_{\text{SRS}}(\Phi=0)$, is that of the linearly most unstable SRS-driven mode. For this mode, the linear value of α_d is larger than unity which implies that $\omega_{\text{SRS}}(0)$ is larger than the linear frequency, $\omega_{\text{free}}(0)$, of a free EPW with the same $k\lambda_D$. As will be proven below, α_d quickly converges towards unity when Φ increases. As a result, $\omega_{\text{SRS}}(\Phi)$ quickly drops towards $\omega_{\text{free}}(\Phi)$, which makes $\delta\omega_{\text{SRS}}$ decrease more rapidly with Φ than $\delta\omega_{\text{free}}$, especially when Φ is small. Since the linear value of α_d increases with $k\lambda_D$, so does the discrepancy between $\delta\omega_{\text{SRS}}$ and $\delta\omega_{\text{free}}$.

In order to test the accuracy of our theoretical estimate, $\delta\omega_{\text{SRS}}$, we compare it with the frequency shift $\delta\omega_{\text{num}}$ measured from Vlasov–Maxwell simulations of SRS. The simulations are performed with the Eulerian Vlasov code ELVIS.^{6,7} The space and time steps are $\Delta x/\lambda_l = c\Delta t/\lambda_l = 0.03$. The velocity step varies from run to run, with $0.0016 \leq \Delta v/v_{Te} \leq 0.015$, where $v_{Te} \equiv (T_e/m_e)^{1/2}$ is the thermal speed. The density profile is finite, with a central, flat region from $x/\lambda_l = 28$ to 242 (see Fig. 1 of Ref. 7). The laser enters from vacuum on the left ($x=0$), and a small-amplitude seed scat-

^{a)}Electronic mail: didier.benisti@cea.fr

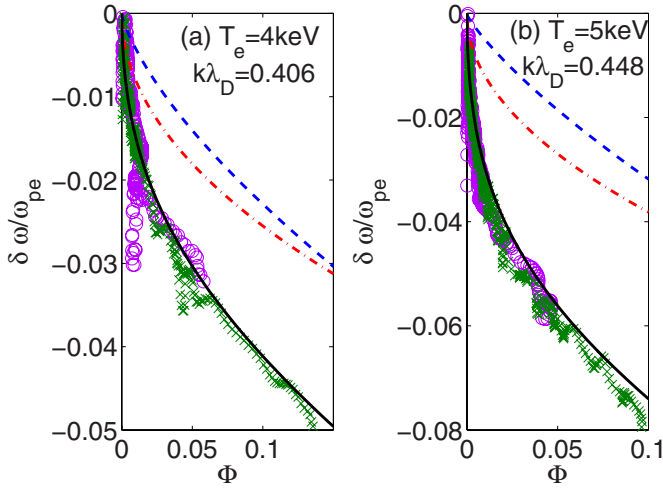


FIG. 1. (Color online) $\delta\omega_{\text{srs}}$ (black solid line), $\delta\omega_{\text{free}}$ (blue dashed line), $\delta\omega_D$ (red dot-dashed line), $\delta\omega_{\text{num}}$ at $x=77\lambda_l$ (purple circles) and at $x=193\lambda_l$ (green crosses) for $I_l=2 \text{ PW/cm}^2$ and (a) $T_e=4 \text{ keV}$, and (b) $T_e=5 \text{ keV}$.

tered light wave is injected on the right with λ_s chosen to match the frequency of the most unstable mode. Our simulations are thus more easily related to optical mixing or Raman amplification than to SRS growing from noise. The seed intensity varied from $I_s/I_l=10^{-5}$ to 10^{-8} , without affecting the dispersion relation. $\delta\omega_{\text{num}}$ and Φ are obtained via the Hilbert transform (see, e.g., Ref. 8) of the electrostatic field E_x versus time at one x . k is computed from the distance between zero-crossings of E_x . The scattered wave number and frequency are found similarly.

As illustrated in Figs. 1 and 2, we always find an excellent agreement between $\delta\omega_{\text{srs}}$ and $\delta\omega_{\text{num}}$. For all runs, the unperturbed plasma density n_0 is 10% of the critical one, and the laser vacuum wavelength is $\lambda_l=0.351 \mu\text{m}$. The values of

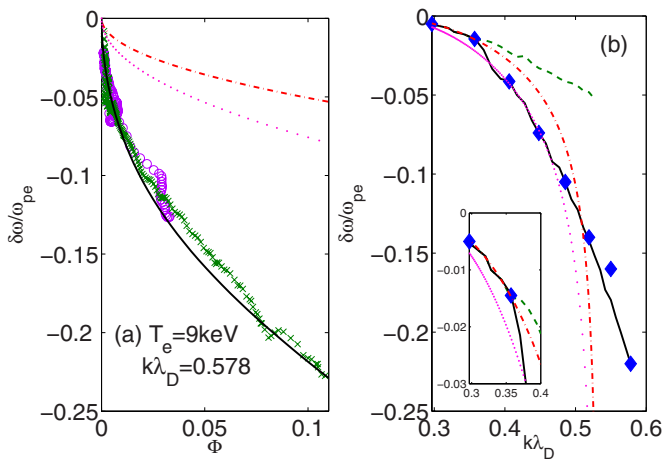


FIG. 2. (Color online) (a) $\delta\omega_{\text{srs}}$ (black solid line), $\delta\omega_D$ (red dot-dashed line), $\delta\omega_{\text{MO}}$ (pink dots), and $\delta\omega_{\text{num}}$ at $x=77\lambda_l$ (purple circles) and at $x=232\lambda_l$ (green crosses) for $T_e=9 \text{ keV}$ and $I_l=8 \text{ PW/cm}^2$. (b) $\delta\omega_{\text{num}}$ (diamonds), $\delta\omega_{\text{srs}}$ (black solid line), $\delta\omega_{\text{free}}$ (green dashed line), $\delta\omega_D$ (red dot-dashed line), and $\delta\omega_{\text{MO}}$ (pink dotted line) vs $k\lambda_D$ when $\Phi=0.1$. Each numerical result is for a distinct run with a different T_e , and $I_l=2 \text{ PW/cm}^2$ for $T_e < 6 \text{ keV}$ ($k\lambda_D < 0.485$), $I_l=4 \text{ PW/cm}^2$ for $T_e=6 \text{ keV}$, $I_l=6 \text{ PW/cm}^2$ for $T_e=7 \text{ keV}$ ($k\lambda_D \approx 0.519$) and $I_l=8 \text{ PW/cm}^2$ for $T_e > 7 \text{ keV}$.

the laser intensity, I_l , and the electron temperature, T_e , are specified in the figure captions. The indicated value of $k\lambda_D$ in these figures refers to the wave number of the linearly most unstable SRS-driven EPW for the given plasma and laser parameters. $\delta\omega_{\text{num}}$ is only plotted before Φ reaches its first local time maximum. After this maximum, and near the laser entrance, one may see pulses in the time evolution of Φ . The good agreement between $\delta\omega_{\text{srs}}$ and $\delta\omega_{\text{num}}$ usually remains for the early pulses (not only for the first one) but eventually breaks down together with the validity of the adiabatic approximation. Away from the laser entrance, we numerically find that Φ increases with time until a sideband eventually grows, which is reminiscent of the result of Brunner and Valeo,² and which then makes the notions of a central frequency, and its shift, irrelevant. For the range of intensities we investigated, $I_l \leq 10 \text{ PW/cm}^2$, and when $0.3 \leq k\lambda_D \leq 0.58$, we thus find that our theory breaks down mainly when, eventually, the EPW can no longer be considered nearly monochromatic. For lower values of $k\lambda_D$, and maybe larger intensities, a nearly monochromatic EPW may reach so large an amplitude that higher harmonics and a “DC” field need to be accounted for in order to correctly calculate the frequency shift, as recently reported in Ref. 12.

We now compare $\delta\omega_{\text{srs}}$ and $\delta\omega_{\text{num}}$ to well-known previously published formulas for the frequency shift, such as the one derived by Dewar⁹ for a free EPW by assuming adiabatic electron motion,

$$\frac{\delta\omega_D}{\omega_{pe}} \equiv \frac{1.09 f_0''(u_\phi) (\omega_{\text{lin}}/\omega_{pe}) \sqrt{\Phi}}{1 + (k\lambda_D)^2 - (\omega_{\text{lin}}/\omega_{pe})^2}. \quad (4)$$

ω_{pe} is the plasma frequency, $f_0(u) \equiv \exp(-u^2/2)/\sqrt{2\pi}$, $f_0'' = d^2 f_0/du^2$, $u_\phi \equiv \omega_{\text{lin}}/(kv_{Te})$, and ω_{lin} is the linear solution of $1 + \text{Re}(\chi) = 0$, χ being calculated by making use of the adiabatic approximation. ω_{lin} only exists, and therefore $\delta\omega_D$ is only defined, when $k\lambda_D < 0.53$. As can be seen in Fig. 2(b), $\delta\omega_D$ yields a good estimate of $\delta\omega_{\text{srs}}$ and $\delta\omega_{\text{num}}$ only when $k\lambda_D \leq 0.35$. Morales and O’Neil¹⁰ derived the frequency shift of a free EPW by assuming that it is suddenly excited and found $\delta\omega_{\text{MO}} \approx (1.63/1.09)\delta\omega_D$. $\delta\omega_{\text{MO}}$ is also only defined when $k\lambda_D < 0.53$ and Fig. 2(b) seems to show that it is close to $\delta\omega_{\text{srs}}$ and $\delta\omega_{\text{num}}$ only when $0.37 \leq k\lambda_D \leq 0.46$. This agreement is fortuitous: the ratio $\delta\omega_{\text{srs}}/\delta\omega_{\text{MO}}$ depends on Φ because $\delta\omega_{\text{srs}}$ is not simply proportional to $\sqrt{\Phi}$. If one were to extrapolate the values of $\delta\omega_D$ and $\delta\omega_{\text{MO}}$ beyond $k\lambda_D = 0.53$ by choosing for ω_{lin} the linear frequency of the SRS-driven wave, $\delta\omega_D$ and $\delta\omega_{\text{MO}}$ would be found to underestimate $\delta\omega_{\text{srs}}$ whenever $k\lambda_D > 0.35$ and $k\lambda_D > 0.4$, respectively. An example of this is given in Fig. 2(a).

We now explain our theoretical solution of Eq. (2) yielding $\delta\omega_{\text{srs}}$. First of all χ , whose derivation is detailed in Ref. 5, is calculated by assuming adiabatic electron motion and by accounting for the change in phase velocity as the wave grows. As for the variations of η , and therefore those of α_d , they are deduced from the envelope equations of the plasma and scattered waves. The envelope equation of the EPW is given by Eq. (5) of Ref. 5 which, at zero order in $k^{-1}\partial_x E_p$, yields

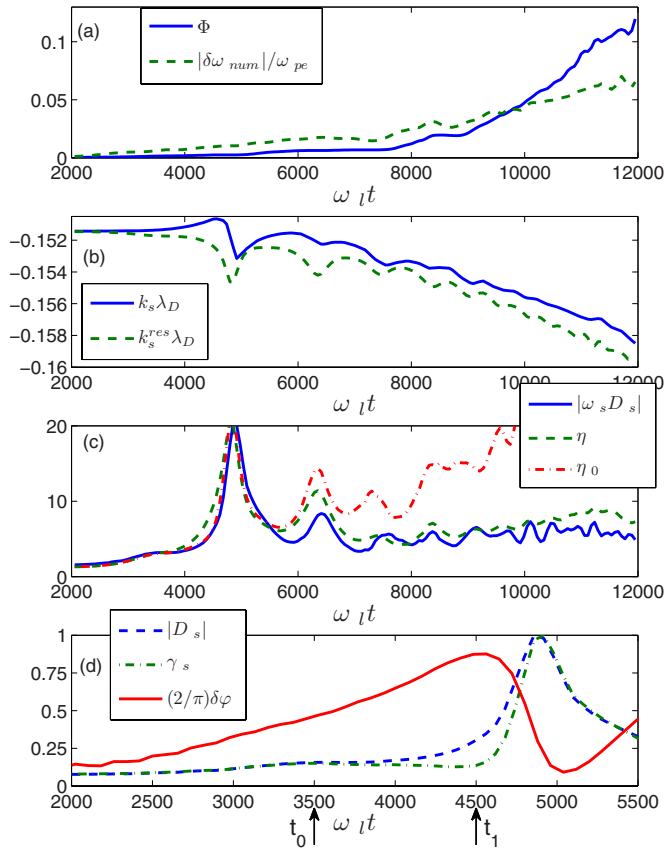


FIG. 3. (Color online) Numerical values for $T_e=5$ keV, $k\lambda_D \approx 0.448$, and $I_l=4$ PW/cm², measured at $x=173.5\lambda_l$ of, panel (a): Φ (blue solid line) and $|\delta\omega_{\text{num}}|$ (green dashed line); panel (b): k_s (blue solid line) and k_s^{res} (dashed green line); panel (c): $|\omega_s D_s|$ (blue solid line), $\eta \equiv E_p/E_d$ (green dashed line) and $\eta_0 \equiv \eta[k_s=k_s^{\text{lin}}]$, normalized to their linear values; panel (d): $|D_s|$ (blue dashed line) and γ_s (green dot-dashed line) normalized to their maximum values, and $(2/\pi)\delta\varphi$ (red solid line) vs $\omega_l t$.

$$\eta = \frac{-\text{Re}(\chi)}{\text{Im}(\chi)} \cos(\delta\varphi) + \sin(\delta\varphi). \quad (5)$$

For the scattered wave, we start with the standard governing equations, namely, the Maxwell–Ampère law, transverse canonical momentum conservation ($\vec{j}_\perp = -ne^2\vec{A}/m$), and Gauss’s law. As usual, we work to leading order in the space and time variations of the envelopes, neglect $\partial_t \omega_s$ and $\partial_x k_s$, and keep only resonant driving terms. The resulting scattered-wave envelope equation is

$$[\partial_t + (k_s c^2/\omega_s)\partial_x + i\Delta_s^{\text{res}}]E_s = \Gamma_0 E_p e^{i\delta\varphi}, \quad (6)$$

where $\Delta_s^{\text{res}} \equiv (\omega_s^2 - k_s^2 c^2 - \omega_{pe}^2)/2\omega_s$ represents detuning of the scattered wave from resonance and $\Gamma_0 \equiv kv_{os}/4$. Defining $\gamma_s \equiv E_s^{-1}[\partial_t E_s + (k_s c^2/\omega_s)\partial_x E_s]$, which represents the SRS growth rate for the scattered wave, Eq. (6) yields

$$D_s E_s = \eta(2\Gamma_0^2/\omega_s)E_p e^{i\delta\varphi}; \quad D_s \equiv \gamma_s + i\Delta_s^{\text{res}}. \quad (7)$$

Assuming $k \approx \text{const.}$ and pump depletion is negligible so that $\Gamma_0 \approx \text{const.}$, Eq. (7) yields $\eta \propto |\omega_s D_s|$. The accuracy of the latter expression is illustrated in Fig. 3(c) which shows similar time evolutions for the numerically measured values of $|\omega_s D_s|$ and η . It is noteworthy that η reaches its maximum

for quite a small value of $\Phi \approx 2.5 \times 10^{-3}$, showing that η quickly increases with Φ .

As ω (and possibly k) vary nonlinearly, ω_s and k_s vary to maintain phase-matching ($\omega_l \approx \omega + \omega_s, k_l \approx k + k_s$). If k_s remains close enough to $k_s^{\text{res}} \equiv -[\omega_s^2 - \omega_{pe}^2]^{1/2}/c$ so that $\Delta_s^{\text{res}} \ll \gamma_s$, then Eq. (7) gives $\delta\varphi \approx 0$. From Eq. (5), the variations of η then closely follow those of $1/\text{Im}(\chi)$. Since we proved in Ref. 5 that, partly due to the decrease of the nonlinear Landau damping rate, $1/\text{Im}(\chi)$ increases with the EPW amplitude, we deduce that so does η . Physically, the increase of $1/\text{Im}(\chi)$ enhances the growth rate γ_s which, when $\delta\varphi \approx 0$, is the main cause for the increase of $|D_s|$ and therefore for that of η . Such a scenario is illustrated in Fig. 3(d) for $t < t_0 \equiv 3500/\omega_l$, when the increase of $|D_s|$ is due to that of γ_s .

Consider the opposite case, where k_s remains approximately constant while ω_s upshifts. This makes Δ_s^{res} , and therefore $|D_s|$ and η , increase. Hence, whether the scattered wave remains on resonance ($k_s \approx k_s^{\text{res}}$) or not, η initially quickly increases with the wave amplitude and α_d therefore converges towards unity.

Numerically, we find an overall decrease of k_s with time (and therefore with Φ), similar to that of k_s^{res} [see Fig. 3(b)]. The variations of k_s somewhat lag behind those of k_s^{res} , and by the time k_s has significantly changed, η has grown enough for α_d to be, and remain, very close to unity. This can be appreciated in Fig. 3(c) where the numerically calculated values of η are compared to those of η_0 derived by assuming that k_s kept its linear value. It is therefore valid to calculate α_d by assuming $k_s = \text{const.}$, which we actually did when deriving $\delta\omega_{\text{SRS}}$.

γ_s may be adequately found by a simpler method than solving Eqs. (5) and (6). For all figures we use $\gamma_s = \sqrt{\gamma_0^2 + \nu_{\text{NL}}^2}/4 - \nu_{\text{NL}}/2$ where the nonlinear Landau damping rate, ν_{NL} , is given by Eq. (49) of Ref. 5, and $\gamma_0 = kv_{os}\omega_{pe}/(4\sqrt{\omega_s\omega})$. This formula for γ_s matches the maximum growth rate of Ref. 11 in the linear regime, and allows for kinetic enhancement due to Landau damping reduction. It however does not account for observed space dependence of γ_s , which may induce space variations in $\delta\omega$, larger at larger laser intensities. There is therefore a limitation in I_l for the validity of our calculation, which increases with $k\lambda_D$. When $0.3 \leq k\lambda_D \leq 0.58$, our theory works well at least up to $I_l = 2$ PW/cm².

Let us now discuss previous results on SRS with the help of Fig. 3, which is representative of all our numerical results. Figure 3(b) shows a constant increase of $\delta\varphi$ towards $\pi/2$ until time $t_1 \approx 4500\omega_l^{-1}$. This is consistent with Eq. (7) since, before t_1 , k_s remains nearly constant while ω_s upshifts by about $-\delta\omega_{\text{SRS}}$, which makes Δ_s^{res} increase compared to γ_s . At time t_1 , k_s quickly approaches k_s^{res} which makes $\delta\varphi$ drop towards 0 and γ_s increase because the driving term for the waves is proportional to $\cos(\delta\varphi)$. Therefore, in agreement with the results of Ref. 1, we do find that the frequency shift induces a detuning, $\delta\varphi$, which slows down the growth of SRS.

However, before time $t_{\text{SB}} \approx 12000\omega_l^{-1}$, $\delta\varphi$ does not vary by more than $\pi/2$ which implies that, before this time, the

waves keep growing despite a large frequency shift, as is clear from Fig. 3(a). At time t_{SB} a sideband develops, which entails large and correlated fluctuations in Φ and $\delta\varphi$. Although we do find bursts in the SRS reflectivity, in none of our simulations could they be attributed to the frequency shift alone. In fact, the impact of the frequency shift on the detuning is strongly limited by a shift in k_s similar to that plotted in Fig. 3(b).

Such a wave number shift is consistent with the spectral streak shown in Ref. 13 (despite having a larger frequency shift than our theory predicts). In this paper it was argued that, because of this streak, the waves should be in the form of pulses moving to the left. We do find that the waves are amplified to the left and that SRS keeps on being regenerated inside of the simulation box. However, we have not recovered a spatially well-isolated pulse as in Ref. 13 in the runs presented in this Letter. Unlike in Ref. 13, we have used a Vlasov code with boundary seeding and uniform laser intensity, and have not accounted for sideloss. Preliminary comparisons between PIC simulations with a uniform intensity and Vlasov simulations accounting for a nonuniform intensity and transverse losses seem to indicate that more isolated pulses result from a more peaked intensity. A more detailed study is however left for future work.

We now discuss the results of Refs. 3 and 4, that there exists a maximum amplitude, Φ_{max} , beyond which $1 + \text{Re}(\chi)$ is never 0 and actually increases with Φ , which implies that the SRS growth rate drops when $\Phi > \Phi_{\text{max}}$. This “loss of resonance” scenario therefore yields an estimate of Φ for Raman saturation. However, Fig. 1(b) clearly shows that a quasimonochromatic wave can exist beyond the value $\Phi_{\text{max}} = 0.05$ predicted by Rose⁴ for the loss of resonance when $k\lambda_D = 0.448$. Since we both theoretically and numerically find $|\alpha_d - 1| < 1\%$ when $\Phi > 0.05$, we conclude that $1 + \text{Re}(\chi) \approx 0$ and that the EPW experiences no saturation due to a loss of resonance even when $\Phi > \Phi_{\text{max}}$. Moreover, for the parameters of Fig. 2(a), we find $|\alpha_d - 1| < 2\%$ when $\Phi > 3 \times 10^{-3}$, which demonstrates that an EPW can be driven very close to resonance even when $k\lambda_D > 0.53$ and $\Phi_{\text{max}} = 0$. As noted in Ref. 5, the discrepancy between the numerical

results and the Rose and Russell predictions is mainly due to their assuming that the wave frame is inertial when calculating χ . It is noteworthy that in his famous paper on wave breaking, Coffey¹⁴ also assumed that the wave frame is inertial. Coffey’s criterion would then predict that in the case of Fig. 2(a) the wave would break when $\Phi > 0.03$, which is not the case.

In conclusion, we theoretically derived and solved the nonlinear dispersion relation of an SRS-driven EPW, and found results in very good agreement with those obtained from Vlasov–Maxwell simulations of SRS, whatever the value of $k\lambda_D$ investigated. We moreover showed that the frequency shift of a freely propagating EPW is significantly smaller than that of an SRS-driven EPW when $k\lambda_D \geq 0.35$. We also showed that the scattered electromagnetic wave is initially driven off-resonance as the EPW frequency decreases, which entails a phase shift between the plasma wave and the laser drive, and limits the growth of SRS.

D.J.S. thanks R. R. Lindberg, H. A. Rose, E. A. Williams, and the LLNL laser-plasma theorists for fruitful discussions.

Work at LLNL was performed under the U.S. Department of Energy Contract No. DE-AC52-07NA27344.

¹H. X. Vu, D. F. DuBois, and B. Bezzerides, *Phys. Plasmas* **9**, 1745 (2002).

²S. Brunner and E. J. Valeo, *Phys. Rev. Lett.* **93**, 145003 (2004).

³H. A. Rose and D. A. Russell, *Phys. Plasmas* **8**, 4784 (2001).

⁴H. A. Rose, *Phys. Plasmas* **10**, 1468 (2003).

⁵D. Bénisti and L. Gremillet, *Phys. Plasmas* **14**, 042304 (2007).

⁶D. J. Strozzi, M. M. Shoucri, and A. Bers, *Comput. Phys. Commun.* **164**, 156 (2004).

⁷D. J. Strozzi, E. A. Williams, A. B. Langdon, and A. Bers, *Phys. Plasmas* **14**, 013104 (2007).

⁸R. Jha, D. Raju, and A. Sen, *Phys. Plasmas* **13**, 082507 (2006).

⁹R. L. Dewar, *Phys. Fluids* **15**, 712 (1972).

¹⁰G. J. Morales and T. M. O’Neil, *Phys. Rev. Lett.* **28**, 417 (1972).

¹¹J. F. Drake, P. K. Kaw, Y. C. Lee, G. Schmidt, C. S. Liu, and M. N. Rosenbluth, *Phys. Fluids* **17**, 7787 (1974).

¹²R. R. Lindberg, A. E. Charman, and J. S. Wurtele, *Phys. Plasmas* **14**, 122013 (2007).

¹³H. X. Vu, L. Yin, D. F. DuBois, B. Bezzerides, and E. S. Dodd, *Phys. Rev. Lett.* **95**, 245003 (2005).

¹⁴T. P. Coffey, *Phys. Fluids* **14**, 1402 (1971).